# Transcriptional induction of Periostin by a Sulfatase 2-TGFβ1-SMAD signaling axis mediates tumor angiogenesis in hepatocellular carcinoma

Gang Chen[1,2*], Ikuo Nakamura[1*], Renumathy Dhanasekaran[1*], Eriko Iguchi[3*], Ezequiel J. Tolosa[3*], Paola A. Romecin[3], Renzo E. Vera[3], Luciana L. Almada[3], Alexander Miamen[1], Roongruedee Chaiteerakij[1,4], Mengtao Zhou[2], Michael K. Asiedu[1], Catherine D Moser[1], Shaoshan Han[1], Chunling Hu[1], Bubu Banini[1], Abdul M. Oseini[1], Yichun Chen[1], Yong Fang[1], Dongye Yang[1], Hassan M. Shaleh[1], Shaoqing Wang[1] Dehai Wu[1], Tao Song[1], Ju-Seog Lee[5], Snorri S Thorgeirsson[6], Eric Chevet[7], Vijay H. Shah[1], Martin E. Fernandez-Zapico[1, 3], Lewis R. Roberts[1]

[1]Division of Gastroenterology and Hepatology, Mayo Clinic College of Medicine, Rochester, Minnesota, USA

[2]Division of Hepatobiliary Surgery, The First Affiliated Hospital of Wenzhou Medical University, Wenzhou, Zhejiang, China

[3]Schulze Center for Novel Therapeutics, Mayo Clinic, Rochester, Minnesota, USA

[4]Department of Medicine, Faculty of Medicine, Chulalongkorn University and King Chulalongkorn Memorial Hospital, Thai Red Cross Society, Bangkok, Thailand

[5]Department of Systems Biology, MD Anderson Cancer Center, Houston, Texas, USA

[6]Laboratory of Experimental Carcinogenesis, National Cancer Institute, Bethesda, Maryland, USA

[7]Oncogenesis, Stress & Signaling ER440, Label INSERM, Université Rennes-1, Centre de Lutte Contre le Cancer - Eugene Marquis, Rennes, France

[*]These authors contributed equally to this work.

***Running Title**: Role of Sulfatase 2 in HCC progression*

**Correspondence:**

Lewis R. Roberts, M.B. Ch.B., Ph.D. (Corresponding Author)

Division of Gastroenterology and Hepatology,

Mayo Clinic College of Medicine,

200 First Street SW, Rochester, MN 55905

roberts.lewis@mayo.edu

Phone: 507-538-4877; Fax: 507-284-0762

**Grant Support**

This work was supported by National Institutes of Health Grants CA128633 to L.R. Roberts and CA165076 to L.R. Roberts and M.E. Fernandez-Zapico; the Mayo Clinic Center for Cell Signaling in Gastroenterology (NIDDK P30DK084567) to L.R. Roberts and M.E. Fernandez-Zapico; the Mayo Clinic Cancer Center (CA15083) to L.R. Roberts; the Mayo Clinic Center for Translational Science Activities (NIH/NCRR CTSA Grant Number UL1 TR000135) to L.R. Roberts and the National Natural Science Foundation of China 81201953 to G Chen. Its contents are solely the responsibility of the authors and do not necessarily represent the official views of the NIH.

**Keywords:** Sulfatase 2, Periostin, tumor microenvironment, liver cancer, angiogenesis

*The authors have declared that no conflict of interest exists.*

**Abbreviations:** AKT, protein kinase B; Ang1, angiopoietin 1; Ang2, angiopoietin 2, α-SMA, alpha smooth muscle actin; BRAF, proto-oncogene B-Raf; c-KIT, proto-oncogene c-Kit; DEN, diethylnitrosamine; DAPI, 4',6-diamidino-2-phenylindole; ECM, extracellular matrix; ELISA, enzyme-

linked immunosorbent assay; ERK, extracellular signal regulated kinase; FAK, focal adhesion kinase; FGF, basic fibroblast growth factor; GLI1, glioma-associated oncogene 1; HCC, hepatocellular carcinoma; H&E, hematoxylin and eosin stain; HGF, hepatocyte growth factor; HHSECs, human hepatic sinusoidal endothelial cells; HIF-1α, hypoxia-inducible factor 1, alpha; HSPG, heparan sulfate proteoglycan; HS, heparan sulfate; HUVECs, human umbilical vein endothelial cells; KO, knockout; MMP2, matrix metalloproteinase 2; MMP9, matrix metalloproteinase 9; MS, median survival; MVD, microvascular density; OD, optical density; PDGF, platelet-derived growth factor; PDGFA, platelet-derived growth factor A; PDGFB, platelet-derived growth factor B; PDGFRα, platelet-derived growth factor receptor alpha; PDGFRβ, platelet-derived growth factor receptor beta; POSTN, periostin; rh, recombinant human; SDC1, syndecan-1; SHARP, Sorafenib HCC Assessment Randomized Protocol; SMAD2, SMAD family member 2; SULF2, sulfatase 2; Tg, transgenic; TGFβ1, transforming growth factor, beta 1; TKI, tyrosine kinase inhibitor; VCAM-1, vascular cell adhesion molecule 1; VEGFB, vascular endothelial growth factor B; VEGFR1, vascular endothelial growth factor receptor 1; VEGFR2, vascular endothelial growth factor receptor 2; VEGFR3, vascular endothelial growth factor receptor 3; WT, wild type.

**ABSTRACT**

Existing anti-angiogenic approaches to treat metastatic hepatocellular carcinoma (HCC) are weakly effectual, prompting further study of tumor angiogenesis in this disease setting. Here we report a novel role for the sulfatase 2 (SULF2) in driving HCC angiogenesis. Sulf2-deficient mice (*Sulf2* KO) exhibited resistance to diethylnitrosamine-induced HCC and did not develop metastases like wild-type mice (*Sulf2* WT). The smaller and less numerous tumors formed in *Sulf2* KO mice exhibited a markedly lower microvascular density. In human HCC cells, SULF2 overexpression increased proliferation, adhesion, chemotaxis and endothelial tube formation in a paracrine fashion. Mechanistic analyses identified the extracellular matrix protein periostin (POSTN), a ligand of αvβ3/5 integrins, as an effector function in SULF2-induced angiogenesis. POSTN silencing in HCC cells attenuated SULF2-induced angiogenesis and tumor growth in vivo. The TGFβ1-SMAD pathway was identified as a critical signaling axis between SULF2 and upregulation of POSTN transcription. In clinical specimens of HCC, elevated levels of SULF2 correlated with increased microvascular density, POSTN levels and relatively poorer patient survival. Together, our findings define an important axis controlling angiogenesis in HCC and a mechanistic foundation for rational drug development.

## INTRODUCTION

Hepatocellular carcinoma (HCC) is a highly vascular tumor and angiogenesis plays an important role during malignant progression of HCC. Angiogenesis is a process regulated by multiple growth factors, including vascular endothelial growth factor (VEGF), platelet-derived growth factor (PDGF), and basic fibroblast growth factor (FGF) (1). HCCs require new vessel formation both to sustain tumor growth and to facilitate local invasion (2). Tumor cells secrete pro-angiogenic growth factors which induce a self-perpetuating cycle of progressive tumor growth. Drugs targeting angiogenesis have proven to be effective anti-tumor agents in multiple cancers including colorectal cancer and renal cell carcinoma (3, 4). In the case of HCC, traditional chemotherapeutics are not effective treatment options and indeed sorafenib, an antioangiogenic agent, is currently the only drug approved for HCC management (5). Sorafenib is a multi-kinase inhibitor that inhibits VEGF receptors, PDGF receptors, c-KIT, and BRAF. Unfortunately, sorafenib shows only limited effectiveness against advanced HCC and most patients have only modest survival benefit with significant side effects. There is therefore an urgent need to develop more effective anti-angiogenic strategies for HCC derived from a basic understanding of the pathogenesis of this malignancy.

Heparan sulfate proteoglycans (HSPGs) play important roles in cancer progression. HSPGs on the cell surface or in the extracellular matrix act as storage sites for key pro-angiogenic factors including FGF, TGFβ and VEGF. Growth factors also utilize HSPGs as co-receptors for their tyrosine kinase receptors (6-8) Sulfation of particular saccharide moieties of HSPGs is required for growth factor signaling. Sulfatase 2 (SULF2) catalyzes the removal of 6-O-sulfate groups from heparan-sulfate (HS) disaccharide units of HSPGs, decreasing the affinity of HSPGs for heparan-sulfate binding ligands and thus releasing the ligands from sequestration sites and making them available for signaling (9). In our previous study, SULF2 was overexpressed in 60% of human HCCs and was associated with worse prognosis and more rapid recurrence. Further, SULF2 expression promoted proliferation of HCC cells in vitro and correlated

with larger tumor volume and poor survival of nude mice bearing HCC xenografts in vivo (10, 11). Mechanistically, SULF2 enhanced FGF-mediated extracellular signal regulated kinase (ERK) and WNT/β-catenin signaling (10, 12). In this study we define a novel pathway regulated by SULF2, which stimulates angiogenesis in HCC. SULF2 is an enzyme involved in post-translational modification of heparan sulfate proteoglycans (HSPG) by catalyzing the removal of 6-O-sulfate groups from HS disaccharide units of HSPGs, thus modulating the affinity of HSPGs for growth factors and regulating their release and downstream pathway activation. Using a *Sulf2* knockout mouse model, we define a new role for SULF2 in tumor progression of HCC involving the regulation of tumor angiogenesis. Further, we show that the mechanism by which SULF2 modulates angiogenesis is through the up-regulation of POSTN in TGFβ-SMAD dependent manner, an important modulator of angiogenesis in different tumors (13,14). Together the findings of this study propose the SULF2-POSTN axis as a novel target for the development of anti-angiogenic therapies for HCC.

## MATERIALS AND METHODS

A comprehensive list of all the reagents, kits, antibodies and primers used in this study is found in Supplementary Table 1 and Supplementary Table 2.

### Animals

*Sulf2* knockout (*Sulf2*-KO) mice were generated by gene trap insertional mutagenesis (strain name: B6;129P2-Sulf2Gt (PST111)Byg/Mmucd). The homozygous mice were shown to have mild skeletal abnormalities, including premature fusion of the sacral vertebrae and occasional fusion in the sternebrae (15). Homozygous (Hm) KO mice were 13% smaller than their WT littermates at 4 weeks but appeared otherwise normal. Crosses of homozygous mice had lower fecundity than heterozygous crosses. There was no obvious liver abnormality on histology of the Hm KO mouse livers and liver transaminase levels were normal. *Sulf2*-KO mice were crossed with B6;129PF2J mice (catalog No. 100903) from Jackson Laboratory (Bar Harbor, ME, USA) to maintain the strain background. The care and use of the animals for these studies were reviewed and approved by the Mayo Clinic Institutional Animal Care and Use Committee.

### Diethylnitrosamine-induced liver tumor in mice

Diethylnitrosamine (DEN) was used as carcinogen to induce primary liver tumors. DEN is a genotoxic drug and its use has been well established in mouse models for hepatocarcinogenesis (16). At 14 days of age, mice received a single intraperitoneal injection of DEN (15 mg/kg body weight). At 21 days of age, mice were separated by sex and genotyped. Littermates with negative genotypes were used as wild type (WT) controls. Only male mice were included in the analysis as female mice rarely developed tumors with DEN. All mice were sacrificed at 8 months and their liver and lungs examined for tumors. The liver weight, number of visible tumors and size of visible tumors were recorded.

**Analysis of human HCC microarray gene expression data**

HCC tumor and adjacent benign tissues were obtained at surgical resection from 139 individuals at centers in Asia, Europe and the United States. The details of the microarray gene expression profiling were previously reported by Lee et al (17). Kaplan Meier analysis was used to compare overall survival between patients with high versus low POSTN expression. Partek software was used to identify SULF2-associated angiogenic factors.

**TCGA gene expression analysis**

mRNA expression data from HCC specimens (200 tumors; 50 surrounding normal liver tissues) was obtained from The Cancer Genome Atlas (TCGA). The file containing level 3 normalized RSEM (RNA-Seq by Expectation Maximization) data from the Firehose run of the Broad Genome Data Analysis Center was downloaded on Dec 17th 2014 [http://gdac.broadinstitute.org]. Fold change for POSTN transcript was calculated as the ratio of gene expression values of tumor to normal, with the median sample value of normal tissues used as baseline. A ratio of log2 (tumor/normal) greater than or equal to 1.0 (a fold change of tumor vs. normal greater than or equal to 2) was considered increased, and a ratio of log2 (tumor/normal) less than or equal to –1.0 was considered decreased. Spearman analysis was used to analyze correlation between POSTN and SULF2.

**Cell Lines and rhPOSTN and rhTGFβ1 treatments**

Hep3B and PLC/PRF/5 cell lines (SULF2-negative) were obtained from American Type Culture Collection (Manassas, VA, USA) and cultured in complete Minimum Essential Media (MEM) with 10% fetal bovine serum (FBS). Huh-7 cells (SULF2-positive) were obtained from the Japan Health Science Research Resources Bank (HSRRB, Osaka, Japan) and grown in Dulbecco's Modified Eagle's Medium

(DMEM) with 10% FBS. Human hepatic sinusoid endothelial cells (HHSECs) and human umbilical vein endothelial cells (HUVECs) were obtained from ScienCell Research Laboratories (Carlsbad, CA, USA). Both HHSECs and HUVECs were cultured in EGM-2 Culture Medium. Cell Authentication was performed by short tandem repeat (STR) analysis (GENEWIZ, South Plainfield, NJ 07080) based on the Approved American National Standards (ANSI).

For recombinant human POSTN (rhPOSTN) treatments, 20 ng/mL of rhPOSTN was used unless otherwise noted. For recombinant TGFβ1 (rhTFGβ1) treatments, 2-10 ng/mL rhTGFβ1 was added to the cells directly in the medium. For the ChIP assay, Huh-7 cells were incubated with 5 ng/mL rhTGFβ1 in serum-free medium for 1 hour.

**Cell transfection**

A recombinant plasmid expressing full-length human SULF2 cDNA cloned into the pcDNA3.1 expression vector from Invitrogen (Grand Island, NY, USA) was used as a SULF2-expressing plasmid (17). Hep3B cells were grown to 60–80% confluence and transfected with SULF2-expressing plasmid or vector plasmid using FuGENE6 Transfection Reagent from Roche (Indianapolis, IN, USA). Short-hairpin RNAs (shRNAs) cloned into lentivirus vector pLKO.1-puro were chosen from the human library (MISSION TRC-Hs 1.0) and purchased from Sigma-Aldrich (St. Louis, MO, USA). Non-target control shRNAs (pLKO.1 NTC vector, Sigma) contain a hairpin insert that generates siRNAs but contains five-base pair mismatches to any known human gene. The target sequences used for SULF2 shRNA constructs were HW11: CAAGGGTTACAAGCAGTGTAA and HW13: CCACAACACCTACACCAACAA. Lentivirus particles were produced by transient transfection of these two different shRNAs targeting HSulf-2 (pLKO.1-HSulf-2) (shSULF2) and pLKO.1 NTC (scrRNA) along with packaging vectors (pVSV-G and pGag/pol) in 293T cells as previously described (18). Huh-7 cells were grown to 80% confluence and infected with lentivirus particles. Small interfering RNAs (siRNAs) targeting POSTN (siPOSTN) from

Santa Cruz (Santa Cruz, CA, USA) were transfected following the manufacturer's protocol. Non-targeting siRNAs (control siRNA) from Santa Cruz (Santa Cruz, CA, USA) were utilized as a negative control.

**Production of Conditioned Media (CM)**

Hep3B cells transfected with SULF2-expressing plasmid or empty vector plasmid and Huh-7 cells infected with lentivirus containing shSULF2 or scrRNA for 48 hours were grown to 70%-80% confluency and washed 3 times with phosphate buffered saline (PBS) and then incubated in fresh media containing 0.5% FBS for 48 hours. Conditioned media (CM) were harvested, centrifuged at 1000 rpm for 10 minutes to remove cell debris, filtered through a 0.22-μm filter and stored at 4°C. Hep3B cells were also co-transfected with SULF2 and siPOSTN or control siRNA and their CM were harvested.

**Co-culture experiments**

SULF2-downregulated Huh-7 and SULF2-overexpressing Hep3B cells and their respective controls were seeded in 6-well co-culture dishes. HHSECs and HUVECs were cultured on 0.4-μm pore size cell culture inserts from BD Biosciences (San Jose, CA, USA) for 24 hours at $1\times10^5$ cells/well and then maintained in medium containing 0.5% FBS. Inserts were placed in the insert companion plate for 48 hours, which allow diffusion of media components but prevent cell migration. Independent experiments were carried out at least three times.

**RNA extraction and Quantitative real-time PCR analysis**

Total RNA was extracted using RNAeasy mini Kit (Qiagen, CA, USA). cDNA synthesis was performed using High Capacity cDNA Reverse Transcription kit from Applied Biosystems (Grand Island, NY, USA) to transcribe 2 μg of total RNA. mRNA levels were quantified by real-time reverse transcrip-

tion polymerase chain reaction (RT-qPCR) in ABI 7300 system. Each mRNA level was normalized by comparison to 18S ribosomal RNA in the same samples. All reactions were performed in triplicate. Primer sequences are listed in Supplementary Table 2.

**Western blot analysis**

Whole cell lysates and tissues from mice were extracted in lysis buffer and quantified using BCA protein assay kit (Pierce, IL, USA). Equal amounts of protein (20 μg/lane) were separated on 4-15% sodium dodecyl sulfate-polyacrylamide gel electrophoresis and then transferred to polyvinylidene fluoride membranes (Millipore, MA, USA). After blocking for 1 hour with 5% BSA and washing with TBST, the membranes were probed with polyclonal or monoclonal antibodies against SULF2, POSTN, phospho-FAK, FAK, phospho-AKT, AKT and β-actin by incubation at 4°C overnight. Subsequently, goat anti-mouse or goat anti-rabbit horseradish peroxidase-conjugated secondary antibodies were used to detect antigen antibody complexes. Immune complexes were visualized using the HyGLO HRP detection kit from Denville scientific (Metuchen, NJ, USA) and exposed to X-ray films. β-actin was used to control for equal loading. Each experiment was repeated at least 3 times.

**Immunohistochemical staining**

For immunohistochemical (IHC) staining, tumor tissues were fixed in formalin, embedded in paraffin, cut into 4 μm sections and stained with antibody against CD31 and VEGFR2. Negative controls were set up by replacement of the primary antibody with 1% BSA-TBS. For quantification of tumor microvascular density (MVD), CD31-positive cells were identified by a brown precipitate in the cytoplasm of endothelial cells; vessels in each section were counted in five microscope fields (19).

**Immunofluorescence (IF) staining and confocal microscopy**

Frozen sections of tumor tissues from either *Sulf2*-KO or WT mice were permeabilized with 0.1% Triton X-100 in PBS for 30 minutes. Sections were then blocked for 1 hour at room temperature with 5% goat serum and incubated with anti-heparan sulfate (HS) antibody (RB4EA12) overnight at 4°C. Sections were then rinsed in PBS and incubated with Alexa Fluor 594–conjugated anti-rabbit IgG from Invitrogen (Carlsbad, CA, USA) for 1hour at room temperature. The content of sulfated disaccharides was validated using High Performance Liquid Chromatography (HPLC) as previously described. Disaccharide peaks were identified by reference to the consistent elution positions of authentic disaccharide standards.

HHSECs and HUVECs were seeded on 8-well culture slides and incubated for 48 hours with conditioned media from Huh-7 cells infected with scrRNA or shSULF2, Hep3B cells transfected with empty vector or SULF2 and Hep3B cells transfected with siPOSTN or control siRNA. Cells were rinsed with PBS at room temperature and fixed for 20 minutes with 2.5% formaldehyde in piperazine-N,N′-bis(2-ethanesulfonic acid) (PIPES). They were then rinsed with PBS and blocked with 5% normal goat serum for 1 hour at 37°C. After incubation with antibody against POSTN, p-FAK, p-AKT, VEGFB, MMP2, MMP9, PDGFA and PDGFB for 1 hour at 37°C, they were rinsed in PBS and incubated with Alexa Fluor 488–conjugated anti-mouse from Molecular Probes (Grand Island, NY, USA) for 1 hour at room temperature, subsequently mounted with Prolong Gold anti-fade reagent with DAPI from Invitrogen (Carlsbad, CA, USA). Slides were examined by confocal microscopy (Zeiss LSM-510).

**Enzyme-linked immunosorbent assay (ELISA)**

TGFβ1 concentrations were measured using a human TGFβ1 immunoassay kit from Abcam (Cambridge, MA, USA). POSTN concentrations were measured using a human POSTN immunoassay kit from MyBioSource (San Diego, CA, USA). Samples were prepared following the manufacturer protocol.

**Cell proliferation, chemotaxis, and adhesion assays**

HHSECs ($1\times10^3$) and HUVECs ($2\times10^3$) cells were seeded in a 96-well culture plate for 3 hours and washed 3 times with PBS. After confirmation of cellular adhesion to the plates, the medium was replaced with each CM. Different concentrations of recombinant human POSTN (rhPOSTN) and siPOSTN were also used to treat HHSECs and HUVECs. Twenty-four, 48 and 72 hours after treatment, endothelial cell viability was determined using 3-(4,5-dimethylthiazol-2-yl)-2,5-diphenyl tetrazoliumbromide (MTT) assays from ATCC (Rockville, MD, USA). The absorbance was determined at 570 nm. Experiments were carried out in triplicate.

The chemotaxis of endothelial cells to different CM was measured by Transwell assay. HHSECs ($5\times10^4$) or HUVECs ($5\times10^4$) in 500 μL serum-free medium were added into 24-well chambers with 8-μm pore size from BD Biosciences (San Jose, CA, USA). Then 750 μL of each CM supplemented with 0.5% FBS were used as a chemo-attractant in the lower compartment. After 24-hour culture at 37 °C, the migrated cells, adhering to the lower surface of the membrane, were fixed with 100% methanol, stained with crystal violet and counted under a light microscope. Migrated cells were counted in five randomly selected microscopic fields for each chamber and chemotaxis was expressed as the number of migrated cells per field. Each experiment was performed in triplicate.

For measurement of cell adhesion, HHSECs and HUVECs were cultured in CM for 12 hours and resuspended in respective CM at a density of $2\times10^5$ cells/mL, followed by addition of 100 μL cell suspension to each well of 96-well plates. Following incubation for 1 hour at 37°C, unattached cells were removed by rinsing twice with PBS. Cells were then stained with Crystal Violet for 10 minutes. Plates were read at 570 nm. Different concentrations of rhPOSTN and siRNA were also used to treat HHSECs and HUVECs. Each experiment was performed in triplicate.

**Xenografts model and adenovirus infection protocol**

Hep3B cells ($1.75\times10^6$) were seeded in MEM medium supplemented with 10% FBS and cultured overnight. For the infection, adenoviruses were obtained from Vector BioLabs (Malvern, PA, USA) and used at concentrations suggested by the manufacturer. Four experimental groups were design: 1) Ad-CMV-Null:Ad-GFP-U6-scrmb-shRNA (Empty vector + scrRNA); 2) Ad-h-SULF2:Ad-GFP-U6-scrmb-shRNA (SULF2 + scrRNA); 3) Ad-CMV-Null:Ad-GFP-U6-h-POSTN-shRNA (Empty vector + shPOSTN); 4) Ad-h-SULF2: Ad-GFP-U6-h-POSTN-shRNA (SULF2 + shPOSTN). In all the groups, the ratio between the SULF2 overexpressing adenovirus and the adenovirus used to knockdown POSTN was of 0.5:1.5, respectively. The efficiency of SULF2 overexpression and POSTN knockdown was tested by RT-qPCR and Western immunoblotting (data not shown). Seventy-two hours after infection, cells were harvested by trypsinization, washed with PBS and reconstituted with matrigel (1:10) (BD Biosciences) in MEM medium to a final volume of 0.1 mL/mouse. Twenty-four 4–5 week old male NOD/SCID mice were injected subcutaneously in the right flank (at sacroiliac joint level) with $5\times10^6$ adenovirus-infected Hep3B cells/mouse. Tumor growth was monitored three times a week and measured using a digital Vernier caliper to calculate the tumors volume (V=(a x b2)/2). Mice were cared for and handled in accordance with institutional and National Institutes of Health guidelines and after 40 days were sacrificed and tissue collected.

**Cell tube formation assay**

Evaluation of tube formation by endothelial cells was performed using In Vitro Angiogenesis Assay Kit from Millipore (Temecula, CA, USA). Briefly, ECMatrix gel solution was thawed, mixed with diluent buffer, and placed in a precooled 96-well plate. The plate was then placed at 37°C for 1 hour to enable the matrix solution to gel. HHSECs and HUVECs were cultured in CM for 12 hours and resuspended in respective CM at a density of $2\times10^5$ cells/mL. 100 µL of the cell suspension was loaded onto the surface of the gelled matrix and incubated at 37°C for 6 hours. Images were acquired using Zeiss Axi-

oplan 2 (bright-field, ×100) with attached Zeiss Axiocam and Axio Vision 4.6.3 software, and tubule length was measured using Image J image analysis software from NIH (Bethesda, MD, USA). Different concentrations of rhPOSTN and siPOSTN were also used to treat HHSECs and HUVECs. Each experiment was performed in triplicate.

**Immunoprecipitation**

Huh7 and Hep3B cells grown in 10-cm dishes were washed twice with ice-cold phosphate-buffered saline (PBS) and lysed on ice for 10 minutes in 1 mL of radioimmunoprecipitation assay (RIPA) lysis buffer with protease inhibitor. Cellular debris was removed by centrifugation at 10,000g for 10 minutes. The supernatant was transferred to a new tube, and 1 mg of mouse IgG and 20 mL volume of resuspended Protein A/G Plus-Agarose Sepharose added (Santa Cruz, CA, USA). After incubation for 30 minutes on ice, the beads were pelleted by centrifugation at 25,000 rpm for 5 minutes at 4°C, and the supernatant was transferred to a new tube. The protein concentration was measured and diluted to approximately 100 mg/mL of total cell protein with PBS. The lysate was incubated with 10 mL of mouse anti-TGFBR3 antibody on ice for 1 hour, and TGFBR3 protein was immunoprecipitated by Protein A/G PLUS-Agarose Sepharose (20 mL) overnight at 4°C. Immune complexes were pelleted by centrifugation for 5 minutes at 1,000g at 4°C, washed 4 times with RIPA buffer, and eluted from the beads by boiling in 40 mL of 1´ sample buffer for 3 minutes. About 20 mL of the sample was analyzed by sodium dodecyl sulfate polyacrylamide gel electrophoresis. Western immunoblot analysis was performed using anti-TGFβ1 and anti-TGFBR3 antibodies.

**Chromatin immunoprecipitation (ChIP) assay**

ChIP was conducted as previously described (20). Briefly, 1 hour after TGFβ1 treatment, Huh-7 cells ($10x10^6$) were cross-linked with 1% formaldehyde, followed by cell lysis. DNA was sheared using a Bioruptor 300 (Diagenode, Denville, NJ) to fragment DNA to ~600 bp. Aliquots of the sheared chromatin were then immunoprecipitated using magnetic beads and a SMAD3 antibody or a normal rabbit IgG. Following immunoprecipitation, cross-links were removed, and immunoprecipitated DNA was purified using spin columns and subsequently amplified by quantitative PCR. PCR primers were designed to amplify regions of the POSTN promoter containing potential SMAD binding sites. The sequences of the primers are listed in Supplementary Table 2. Samples for quantitative SYBR PCR were performed in triplicate using the C1000 Thermal Cycler (Bio-Rad, Hercules, CA). Results are represented as Percentage of Input.

**Statistical Analyses**

All data represent at least three independent experiments using cells from separate cultures and are expressed as the mean ± SEM. Chi square test was used to compare categorical variables and Student's t test was used to compare continuous variables. Differences between the Kaplan-Meier curves of HCC patients with up-regulated and down-regulated SULF2 expression in their initial HCC tissue as compared to the adjacent benign tissue were analyzed using the Log Rank and Wilcoxon test. P values of less than 0.05 were considered to be statistically significant.

## RESULTS

### *SULF2 loss impairs DEN-induced HCC*

To define the role of *Sulf2* in a biologically relevant HCC model, we generated a *Sulf2*-KO mouse. Heterozygous (Hz) KO mice were crossed with each other and progeny were given a single intraperitoneal injection of DEN on day 14 (Supplementary Figure 1A). On day 21, the mice were separated by sex, genotyped and RT-qPCR was used to confirm that the expression of *Sulf2* was progressively and significantly lower in Hz KO and homozygous (Hm) KO mice compared to *Sulf2* WT mice ($P<0.001$, Supplementary Figure 1B). Western immunoblotting was also used to confirm knockdown of *Sulf2* protein expression in both the normal liver and tumor cells (Supplementary Figure 1C). We used an anti-heparan sulfate (HS) antibody (RB4EA12) detecting 6-O-sulfated HSPG to confirm the functional consequences of *Sulf2* inactivation in the liver. As expected, *Sulf2* Hm KO mice had higher levels of 6-O-sulfated HSPGs than *Sulf2* Hz KO or *Sulf2* WT mice (Supplementary Figure 1D). Analysis of liver heparan sulfate glycosaminoglycans (HSGAGs) by purification, digestion to their constituent disaccharides, and high-performance liquid chromatography (HPLC) confirmed that liver tissue from *Sulf2* Hz KO mice had higher levels of 6-O-sulfated HSPGs compared to *Sulf2* WT mice (Supplementary Figure 1E).

Assessment of the phenotype of *Sulf2* inactivation on DEN-induced liver tumorigenesis revealed that compared to *Sulf2* WT mice (n=13), *Sulf2* Hz KO mice (n=11) had substantially fewer and smaller tumors, and *Sulf2* Hm KO mice (n=10) had the fewest and smallest tumors (Figure 1A, Supplementary Figure 2A). Hematoxylin-eosin staining showed the typical features of HCC in all 3 groups with enlarged round hyperchromatic nuclei, high nuclear-cytoplasmic ratios, and moderate micro- or macrovesicular fat globules in the cytoplasm (Figure 1B). Significantly smaller proportions of Hm and Hz KO mice had ≥5 tumors/mouse and tumor volume ≥35 $mm^3$ compared with WT mice ($P<0.01$ in Hm KO and $P<0.05$ in Hz KO, Figure 1C). *Sulf2* Hm KO mice also had significantly lower body weight and liver weight than WT mice (Supplementary Figure 2B). Tumor incidence was not different between the three groups (Sup-

plementary Figure 2B). Also, we found that 23% (3/13) of the *Sulf2* WT and 17% (2/11) of the Hz KO mice developed lung metastases, in contrast, none of the Hm KO mice had lung metastases ($p<0.05$) (Figure 1D).

***SULF2 promotes angiogenesis in HCC***

The above findings provide strong evidence for a role of *Sulf2* in HCC tumor progression. Since angiogenesis is considered to be crucial for tumor growth and dissemination, we then evaluated the influence of *Sulf2* on angiogenesis. To this end, liver tumors generated in *Sulf2* Hm KO mice were examined by immunohistochemistry for the endothelial cell marker CD31 followed by calculation of microvascular density (MVD). HCCs from *Sulf2* Hm KO mice had lower MVD than tumors from *Sulf2* WT mice ($P<0.001$, Figure 2A). Similar to CD31, expression of the angiogenic marker VEGFR2 showed down-regulation in tumors from *Sulf2* Hm KO mice compared to *Sulf2* WT animals (Figure 2B).

Tumor angiogenesis involves the proliferation and migration of endothelial cells. Hence, we examined whether these cellular functions were affected by SULF2 in a paracrine manner with *in vitro* experiments. Hep3B cells, which are constitutively low SULF2 expressing cells, were transfected with control vector or SULF2, and Huh-7 (high SULF2 expressing cells) were transfected with scrambled shRNA (scrRNA) or SULF2 shRNA (shSULF2). Conditioned media (CM) from above cells were used to treat human hepatic sinusoidal endothelial cells (HHSECs) and human umbilical vein endothelial cells (HUVECs). Tube formation and chemotaxis of HHSECs and HUVECs were increased after treatment with CM from high SULF2-expressing HCC cells (Hep3B SULF2), compared to CM from low SULF2-expressing cells (Huh-7 shSULF2), ($P<0.05$ for tube length except HUVEC treated with Huh-7-derived CM ($P<0.01$), $P<0.001$ for chemotaxis except HHSEC treated with Hep3B-derived CM ($P<0.01$), Figure 2C and 2D). Similarly, viability and adhesion of HHSECs and HUVECs increased after treatment with CM from high SULF2-expressing HCC cells compared to control cells ($P<0.01$ except HUVEC viability

under Hep3B-derived CM ($P$<0.05) and HHSEC adhesion under Hep3B-derived CM ($P$<0.05), Supplementary Figure 3A and 3B). Thus we were able to demonstrate that SULF2 regulates angiogenesis both *in vivo* and *in vitro* by increasing angiogenic potency of endothelial cells.

***SULF2-induced angiogenesis is dependent on POSTN***

To determine the mediators of SULF2-induced HCC angiogenesis, we conducted an *in silico* study to identify potential candidate effectors of this phenomenon (Supplementary Figure 4A). We identified 178 candidate genes selected from 738 publications (Supplementary Table 3 and Supplementary Table 4). We then performed a correlation analysis of these 178 candidates with SULF2 expression in a microarray gene expression analysis of 139 resected human HCCs and identified the top 10 angiogenic factors most significantly correlated with SULF2 expression (Supplementary Figure 4B). We also added 15 well-established angiogenic factors (Supplementary Figure 4C), which were not in the top 10 to create a comprehensive list of 25 pro-angiogenic candidates (17, 21). We then evaluated the expression of these 25 candidates in Hep3B cells overexpressing SULF2 or not and Huh-7 cells transfected with scrRNA or shSULF2. We found that overexpression of SULF2 in Hep3B cells increased expression of 15 of the 25 candidates examined. Among these, POSTN, a pro-angiogenic extracellular matrix protein secreted by tumor or stromal cells (22-24) was the most highly correlated gene, being induced approximately 6-fold by the overexpression of SULF2 ($P$<0.001, Figure 3A). In contrast, down-regulation of SULF2 in Huh-7 cells significantly suppressed POSTN expression ($P$<0.001, Figure 3B). *In vitro,* we confirmed using RT-qPCR ($P$<0.001, Figure 3C), Western blotting (Figure 3D), immunofluorescence (Figure 3E) and ELISA ($P$<0.01, Figure 3F), that SULF2 overexpression in hepatocytes increased POSTN expression and secretion. Analysis of the DEN-induced HCCs showed a 4.1 fold higher expression of POSTN in WT mice compared to *Sulf2* Hm KO mice ($P$<0.01, Supplementary Figure 5A and 5B).

To further study the effect of SULF2 on POSTN expression in the tumor microenvironment we used an *in vitro* co-culture model of HCC cells with endothelial cells. Co-culture with SULF2-expressing Hep3B cells increased POSTN expression, and subsequently increased levels of phospho-AKT and phospho-FAK, known downstream effector of POSTN(12), in both HHSECs and HUVECs when compared to co-culture with SULF2-negative Hep3B cells. Conversely, suppression of SULF2 expression in Huh7 cells resulted in decreased POSTN expression and decreased levels of phospho-AKT and phospho-FAK in co-cultured HHSECs and HUVECs (Figure 4A and 4C, respectively). Immunofluorescence showed similar results (Figure 4B and 4D). To confirm that the activation of PI3 kinase pathway was indeed POSTN-mediated we co-transfected SULF2-expressing Hep3B cells with either scrRNA or siPOSTN and showed that the previously observed increase in phospho-Akt and phospho-FAK were aborted when POSTN was suppressed (Figure 4A-4D, last 2 columns).

To define if SULF2-induced POSTN expression was required for the activation of endothelial cells, SULF2 was overexpressed in Hep3B cells and the cells were then subsequently co-transfected with either siRNA targeting POSTN or control scrambled siRNA. CM was collected 24 hours later. Treatment of HHSECs and HUVECs with CM from SULF2-expressing Hep3B cells co-transfected with siPOSTN decreased endothelial cell viability ($P<0.05$), adhesion ($P<0.01$), chemotaxis ($P<0.01$ in HHSEC and $P<0.05$ in HUVEC) and tube formation ($P<0.05$ in HHSEC and $P<0.001$ in HUVEC) when compared with CM from SULF2-expressing Hep3B cells co-transfected with control siRNA (Figure 5A). Further analysis using a similar experimental setting in a Hep3B xenograft model showed that inactivation of POSTN impairs SULF2-induced tumor growth (Figure 5B) and vessel density (data not shown).

To further confirm the effect of POSTN on endothelial cells, we directly treated HHSEC and HUVEC cells with recombinant human POSTN (rhPOSTN) and showed that this led to increased angiogenic potency of endothelial cells as assessed by cell viability ($P<0.05$ in HHSEC and $P<0.01$ in HUVEC), adhesion ($P<0.001$) and tube formation assay ($P<0.01$) (Figure 5C).

Given the previous evidence that SULF2 promotes angiogenesis by increasing the expression of several angiogenic factors in HCC (Figure 3A and 3B), we hypothesized that the SULF2-mediated increased expression of angiogenic factors was partly mediated by activation of the POSTN pathway. Therefore, we examined the mRNA expression profile of Hep3B cells after transfection with SULF2 plasmid followed by co-transfection with either siPOSTN or control siRNA. As hypothesized, targeting the POSTN pathway in SULF2-expressing Hep3B cells by transfection with siPOSTN led to a decrease in the mRNA expression of the angiogenic factors VEGFB, MMP2, MMP9, PDGFA and PDGFB ($P<0.001$ for PDGFB, $P<0.01$ for MMP9 and $P<0.05$ for the others, Figure 5D). In summary, these data indicate that POSTN expression is a key mediator of SULF2-dependent angiogenesis.

***SULF2 increases POSTN expression via activation of the TGFβ pathway***

Next, we investigated the mechanism by which SULF2 induces POSTN expression. Since SULF2 acts via the modulation of growth factor-dependent pathways and TGFβ has been reported to transcriptionally induce POSTN (25, 26) we evaluated if SULF2 induced POSTN via activation of the TGFβ pathway. We treated HCC cells with low or high SULF2 expression with TGFβ1 and found that expression of SULF2 in Hep3B cells led to activation of TGFβ1 downstream signaling, as evidenced by increase in phospho-Smad2 and phospho-Smad3 expression, and enhanced TGFβ1-induced POSTN expression (Figure 6A). Similar findings were confirmed by examining POSTN mRNA expression in HCC cells and POSTN protein expression in the CM (Figure 6B). We found by immunocytochemistry and Western immunoblotting higher levels of TGFβ1 and POSTN in SULF2 expressing cells compared with the controls (Figure 6C and 6D). We then explored the mechanism by which SULF2 activates the TGFβ pathway. Of the 3 receptors, TGFBR1, TGFBR2, and TGFBR3/betaglycan, we identified TGFBR3 as a potential target for desulfation by SULF2, as it is an HSPG. TGFBR3 functions as a storage co-receptor

for the TGFβ1 ligand at the cell surface, sequestering the ligand and thus inhibiting TGFβ1 signaling (27). To confirm this effect in HCC cells, Huh-7 cells with low or high SULF2 expression were treated with TGFβ1 and their cell lysates were then immunoprecipitated using antibodies against TGFBR3. This revealed that the interaction between TGFβ1 and TGFβR3 was reduced in SULF2 expressing cells (Figure 6E), likely thus increasing TGFβ1 availability. This hypothesis is further confirmed by ELISA demonstrating that conditioned medium from SULF2 expressing cells had higher concentrations of TGFβ1 in a time dependent manner when compared to parental control vector transfected cells (Figure 6F). After that, we confirmed that SULF2-mediated stimulation of POSTN is TGFβ-dependent by demonstrating that the increase in POSTN expression and secretion in SULF2 expressing cells can be blocked by treating the cells with the TGFβR inhibitor SB431542 (Figure 6G). Finally, we confirmed by ChIP assay that POSTN is downtream of TGFβ1 pathway effector such as Smad3 (Figure 6H). To summarize, we demonstrate that SULF2 promotes the release of TGFβ1 from TGFBR3, thereby leading to activation of the TGFβ pathway, which in turn transcriptionally enhances expression and secretion of POSTN.

***Correlated expression of SULF2 and POSTN in human HCC predicts poor prognosis***

Finally, to determine the translational significance of our findings, we examined the expression of SULF2 and POSTN in human HCCs. We first used microarray data from 139 resected human HCC tumors and showed that SULF2 expression in human HCCs was positively correlated with more than 70 (40%) of the 178 angiogenesis related genes we identified earlier, including VCAM1, PDGFRα, and PDGFRβ (Supplementary Table 3). Further, in tumors highly expressing SULF2, the mRNA levels of the neovascularization markers CD31 and CD34 were higher than in tumors with low SULF2 expression ($P<0.001$ for CD31 and $P<0.05$ for CD34, Figure 7A). Thus SULF2 expression appears to be associated with angiogenesis in human HCCs. Also, a subset of human HCCs overexpressed POSTN (Figure 7B,

right panel) and POSTN expression was positively correlated with SULF2 ($P$<0.002, Figure 7B, left panel). Survival analysis showed that patients with HCC tumors expressing high levels of POSTN had a significantly worse prognosis than those with low POSTN expression ($P$= 0.01, Figure 7C). To validate these findings, we used an independent dataset of 200 HCC tumors and 50 peritumoral benign liver tissues from The Cancer Genome Atlas (TCGA) project. The details of analysis are described in MATERIALS AND METHODS. We were able to confirm that POSTN was indeed significantly overexpressed in human HCC tumor tissue when compared to surrounding normal liver and that POSTN expression significantly positively correlated with SULF2 expression ($P$<0.0001, Figure 7D). Also, high POSTN expression was confirmed to be associated with poorer overall survival ($P$=0.002, Figure 7E). Thus we show that in human HCC, SULF2 and POSTN appear to be co-expressed and confer a poor prognosis.

## DISCUSSION

In this study we demonstrated for the first time that SULF2 has a pro-angiogenic role in HCC, one of the major driver of the observed tumor progression. Upon DEN treatment, *Sulf2* HmKO mice had substantially fewer and smaller tumors with absence of lung metastases and lower MVD. We demonstrate that SULF2 expression in the tumor cells enhances the angiogenic potency of endothelial cells in a paracrine fashion thus promoting angiogenesis. Further, our *in-vivo*, *in-vitro* and human HCC data identify POSTN as a novel key downstream mediator of SULF2-dependent angiogenesis and show that RNAi targeting of POSTN in HCC cells attenuates SULF2-induced angiogenesis. Thus we establish the SULF2-POSTN axis as a novel target for development of new anti-angiogenic therapies for HCC.

Angiogenesis is stimulated by the enlarging tumor mass, which secretes pro-angiogenic factors which, in turn, induce the activation and proliferation of endothelial cells in a paracrine fashion, resulting in the sprouting of new vessels from pre-existing ones. SULF2, a heparan sulfate 6-O-sulfatase, releases growth factors from extracellular storage sites and facilitates tumor progression (28-31). But its role in modulating angiogenesis in HCC has not been studied before. In the present study, we examined the role of SULF2 in mediating angiogenesis during HCC progression using *in vitro* and *in vivo* assays. As SULF2 functions by desulfating HSPG chains and thereby regulating the interactions of HSPGs with HS-binding growth factors, cytokines and receptors, we hypothesized that SULF2 mediates the paracrine effects of HCC cells on angiogenesis by regulating the local concentration of angiogenic growth factors in the tumor microenvironment through HSPG desulfation and release of HSPG-bound angiogenic factors on the cell membrane and in the extracellular space. Although results from our previous studies and from other research groups have implicated SULF2 in the regulation of several growth factor signaling pathways, the key downstream pathway mediating SULF2 signaling is still unknown and is likely to be different in different cellular contexts and for different functional effects ( 17, 30, 32).

Through an extensive literature search and *in vitro* experiments, we identified for the first time that POSTN was the most highly regulated downstream angiogenic target of SULF2 in HCC. Up-regulation of SULF2 expression in HCC cells was accompanied by both increased expression and secretion of POSTN, confirming SULF2 can modulate POSTN levels in the extracellular matrix. POSTN is an extracellular matrix protein that is overexpressed in a number of human cancers and has been shown to promote angiogenesis by enhancing the pro-angiogenic potency of endothelial cells (33). In this study, we found down-regulation of POSTN and its downstream signaling substrates phospho-Akt and phospho-FAK in DEN-induced HCCs. Thus, the *in vivo* evidence suggests that POSTN expression and POSTN pathway activation in HCC was SULF2 dependent. Further, using *in vitro* co-culture models, we demonstrate that increased expression of SULF2 stimulates POSTN expression in both HUVECs and HHSECs. Keeping in line with this, we found that SULF2-dependent secretion of POSTN by HCC cells led to activation of POSTN downstream signaling through phospho-FAK and phospho-AKT in endothelial cells. This SULF2-dependent activation of POSTN pathway in the endothelial cells resulted in enhancement of endothelial cell function as measured by endothelial cell viability, adhesion, chemotaxis and tube formation. These effects were confirmed in HUVECs and also shown for the first time in HHSECs, liver specific endothelial cells which exist in the unique liver microenvironment (34). Although POSTN was found to be the most significant downstream mediator of SULF2-dependent angiogenesis, we did find that several other pro-angiogenic factors like VEGFB, MMP-2, MMP-9, PDGFA and PDGFB were also overexpressed in SULF2-expressing cells (Figure 3A and 3B). To further clarify the role of POSTN in the induction of the other angiogenic factors we performed *in vitro* experiments by blocking POSTN expression in SULF2-expressing cells. This resulted in inhibition of the expression of the SULF2-induced angiogenic factors mentioned above, thus suggesting that SULF2 requires POSTN expression to fuel the ongoing production of angiogenic factors, thus promoting angiogenesis of HCC. Activation of this axis ap-

pears to be reflected in patient clinical outcomes, as patients with high POSTN expression in their HCC tumor tissues have substantially worse prognosis.

After the approval of sorafenib for treatment of advanced HCC, there was great hope that other molecular targeted therapies for HCC would soon follow. Unfortunately, thus far, multiple subsequent phase III clinical trials have failed to identify a safe and more effective drug for HCC (35). Hence it is critical to identify novel anti-angiogenic drug targets for treatment of HCC. SULF2 is overexpressed in a majority of HCCs and associated with poor prognosis (36). In view of its ability to regulate multiple angiogenic factors in HCC, SULF2 is likely to be upstream of many of the currently targeted angiogenic pathways. Interestingly, HS mimetic PI-88, an inhibitor of SULF2 function, displays strong anti-angiogenic potency (37). Further this study uses two different datasets to demonstrate for the first time that POSTN is overexpressed in a subset of human HCCs and that patients with high POSTN expression have poor prognosis. Hence both SULF2 and POSTN may serve as biomarkers for more aggressive disease. Consequently inhibition of SULF2-POSTN axis may be a useful therapeutic strategy in combination with other treatments for HCC.

**REFERENCES**

1. Zhu AX, Duda DG, Sahani DV and Jain RK. HCC and angiogenesis: possible targets and future directions. *Nat Rev Clin Oncol* 2011;8:292-301.
2. Bishayee A and Darvesh AS. Angiogenesis in hepatocellular carcinoma: a potential target for chemoprevention and therapy. *Curr Cancer Drug Targets* 2012;12:1095-1118.
3. McCormack PL and Keam SJ. Bevacizumab: a review of its use in metastatic colorectal cancer. *Drugs* 2008;68:487-506.
4. Powles T, Chowdhury S, Jones R, Mantle M, Nathan P, Bex A, et al. Sunitinib and other targeted therapies for renal cell carcinoma. *Br J Cancer* 2011;104:741-745.
5. Llovet JM, Ricci S, Mazzaferro V, Hilgard P, Gane E, Blanc JF, et al. Sorafenib in advanced hepatocellular carcinoma. *N Engl J Med* 2008;359:378-390.
6. Campbell JS, Hughes SD, Gilbertson DG, et al. Platelet-derived growth factor C induces liver fibrosis, steatosis, and hepatocellular carcinoma. *Proc Natl Acad Sci U S A* 2005;102:3389-3394.
7. Ogasawara S, Yano H, Iemura A, et al. Expressions of basic fibroblast growth factor and its receptors and their relationship to proliferation of human hepatocellular carcinoma cell lines. *Hepatology* 1996;24:198-205.
8. Neaud V, Faouzi S, Guirouilh J, et al. Human hepatic myofibroblasts increase invasiveness of hepatocellular carcinoma cells: evidence for a role of hepatocyte growth factor. *Hepatology* 1997;26:1458-1466.
9. Rosen SD, Lemjabbar-Alaoui H. Sulf-2: an extracellular modulator of cell signaling and a cancer target candidate. *Expert Opin Ther Targets* 2010;14:935-949.

10. Lai JP, Oseini AM, Moser CD, et al. The oncogenic effect of sulfatase 2 in human hepatocellular carcinoma is mediated in part by glypican 3-dependent Wnt activation. *Hepatology* 2010;52:1680-1689.
11. Nawroth R, van Zante A, Cervantes S, McManus M, Hebrok M, Rosen SD. Extracellular sulfatases, elements of the Wnt signaling pathway, positively regulate growth and tumorigenicity of human pancreatic cancer cells. *PLoS One*. 2007;2(4):e392.
12. Lai JP, Sandhu DS, Yu C, et al. Sulfatase 2 up-regulates glypican 3, promotes fibroblast growth factor signaling, and decreases survival in hepatocellular carcinoma. *Hepatology* 2008;47:1211-1222.
13. Shao R, Bao S, Bai X, Blanchette C, Anderson RM, Dang T, et al. Acquired Expression of Periostin by Human Breast Cancers Promotes Tumor Angiogenesis through Up-Regulation of Vascular Endothelial Growth Factor Receptor 2 Expression. *Mol Cell Biol* 2004;24:3992-4003.
14. Zhu M, Fejzo MS, Anderson L, Dering J, Ginther C, Ramos L, et al. Periostin promotes ovarian cancer angiogenesis and metastasis. *Gynecol Oncol* 2010;119:337-344.
15. Ratzka A, Kalus I, Moser M, Dierks T, Mundlos S and Vortkamp A. Redundant function of the heparan sulfate 6-O-endosulfatases Sulf1 and Sulf2 during skeletal development. *Developmental dynamics : an official publication of the American Association of Anatomists* 2008;237:339-353.
16. Dhanasekaran R1, Nakamura I, Hu C, Chen G, Oseini AM, Seven ES, Miamen AG, Moser CD, Zhou W, van Kuppevelt TH, van Deursen JM, Mounajjed T, Fernandez-Zapico ME, Roberts LR. Activation of the transforming growth factor-β/SMAD transcriptional pathway underlies a novel tumor-promoting role of sulfatase 1 in hepatocellular carcinoma. *Hepatology*. 2015;61(4):1269-1283.

17. Lee JS, Heo J, Libbrecht L, Chu IS, Kaposi-Novak P, Calvisi DF, et al. A novel prognostic subtype of human hepatocellular carcinoma derived from hepatic progenitor cells. *Nat Med* 2006;12:410-416.
18. Khurana A, McKean H, Kim H, Kim SH, Mcguire J, Roberts LR, et al. Silencing of HSulf-2 expression in MCF10DCIS.com cells attenuate ductal carcinoma in situ progression to invasive ductal carcinoma in vivo. *Breast Cancer Res* 2012;14:R43.
19. de Jong JS, van Diest PJ and Baak JP. Hot spot microvessel density and the mitotic activity index are strong additional prognostic indicators in invasive breast cancer. *Histopathology* 2000;36:306-312.
20. Lo Re, A. E., Fernandez-Barrena, M. G., Almada, L. L., Mills, L., Elsawa, S. F., Lund, G., Ropolo, A., Molejon, M. I., Vaccaro, M. I., and Fernandez-Zapico, M. E. A novel AKT1-GLI3-VMP1 pathway mediates Krasinduced autophagy in cancer cells. *J. Biol. Chem.* 2012; 287:25325–25334
21. Hernandez-Gea V, Toffanin S, Friedman SL and Llovet JM. Role of the microenvironment in the pathogenesis and treatment of hepatocellular carcinoma. *Gastroenterology* 2013;144:512-527.
22. Bao S, Ouyang G, Bai X, Huang Z, Ma C, Liu M, et al. Periostin potently promotes metastatic growth of colon cancer by augmenting cell survival via the Akt/PKB pathway. *Cancer Cell* 2004;5:329-339.
23. Erkan M, Kleeff J, Gorbachevski A, Reiser C, Mitkus T, Esposito I, et al. Periostin creates a tumor-supportive microenvironment in the pancreas by sustaining fibrogenic stellate cell activity. *Gastroenterology* 2007;132:1447-1464.

24. Tilman G, Mattiussi M, Brasseur F, van Baren N and Decottignies A. Human periostin gene expression in normal tissues, tumors and melanoma: evidences for periostin production by both stromal and melanoma cells. *Molecular Cancer* 2007;6:80.
25. Kim JE, Jeong HW, Nam JO, Lee BH, Choi JY, Park RW, Park JY, Kim IS. Identification of motifs in the fasciclin domains of the transforming growth factor-beta-induced matrix protein betaig-h3 that interact with the alphavbeta5 integrin. *J Biol Chem* 2002;277:46159-65.
26. Horiuchi K, Amizuka N, Takeshita S, Takamatsu H, Katsuura M, Ozawa H, Toyama Y, Bonewald LF, Kudo A. Identification and characterization of a novel protein, periostin, with restricted expression to periosteum and periodontal ligament and increased expression by transforming growth factor beta. *J Bone Miner Res* 1999;14:1239-49.
27. Eickelberg O, Centrella M, Reiss M, Kashgarian M, Wells RG. Betaglycan Inhibits TGF-β Signaling by Preventing Type I-Type II Receptor Complex Formation: GLYCOSAMINOGLYCAN MODIFICATIONS ALTER BETAGLYCAN FUNCTION. *Journal of Biological Chemistry* 2002;277:823-829.
28. Neaud V, Faouzi S, Guirouilh J, Le Bail B, Balabaud C, Bioulac-Sage P, et al. Human hepatic myofibroblasts increase invasiveness of hepatocellular carcinoma cells: evidence for a role of hepatocyte growth factor. *Hepatology* 1997;26:1458-1466.
29. Lai JP, Sandhu DS, Yu C, Han T, Moser CD, Jackson KK, et al. Sulfatase 2 up-regulates glypican 3, promotes fibroblast growth factor signaling, and decreases survival in hepatocellular carcinoma. *Hepatology* 2008;47:1211-1222.
30. Lai JP, Oseini AM, Moser CD, Yu C, Elsawa SF, Hu C, et al. The oncogenic effect of sulfatase 2 in human hepatocellular carcinoma is mediated in part by glypican 3-dependent Wnt activation. *Hepatology* 2010;52:1680-1689.

31. Nakamura I, Fernandez-Barrena MG, Ortiz-Ruiz MC, Almada LL, Hu C, Elsawa SF, et al. Activation of the transcription factor GLI1 by WNT signaling underlies the role of SULFATASE 2 as a regulator of tissue regeneration. *J Biol Chem* 2013;288:21389-21398.
32. Uchimura K, Morimoto-Tomita M, Bistrup A, Li J, Lyon M, Gallagher J, et al. HSulf-2, an extracellular endoglucosamine-6-sulfatase, selectively mobilizes heparin-bound growth factors and chemokines: effects on VEGF, FGF-1, and SDF-1. *BMC Biochem* 2006;7:2.
33. Liu AY, Zheng H and Ouyang G. Periostin, a multifunctional matricellular protein in inflammatory and tumor microenvironments. *Matrix Biol* 2014;37:150-156.
34. Van den Eynden GG, Majeed AW, Illemann M, Vermeulen PB, Bird NC, Hoyer-Hansen G, et al. The multifaceted role of the microenvironment in liver metastasis: biology and clinical implications. *Cancer Res* 2013;73:2031-2043.
35. Llovet JM and Hernandez-Gea V. Hepatocellular carcinoma: reasons for phase III failure and novel perspectives on trial design. *Clin Cancer Res* 2014;20:2072-2079.
36. Yang JD, Sun Z, Hu C, Lai J, Dove R, Nakamura I, et al. Sulfatase 1 and sulfatase 2 in hepatocellular carcinoma: associated signaling pathways, tumor phenotypes, and survival. *Genes Chromosomes Cancer* 2011;50:122-135.
37. Joyce JA, Freeman C, Meyer-Morse N, Parish CR and Hanahan D. A functional heparan sulfate mimetic implicates both heparanase and heparan sulfate in tumor angiogenesis and invasion in a mouse model of multistage cancer. *Oncogene* 2005;24:4037-4051.

## FIGURE LEGENDS

***Figure 1. Knockout of SULF2 inhibits HCC progression***.

**A.** Representative images of livers from *Sulf2* WT, *Sulf2* Hz KO and *Sulf2* Hm KO mice, carrying tumors after DEN-treatment. At 14 days of age mice received a single intraperitoneal injection of DEN. All mice were sacrificed at 8 months old and their liver and lungs were examined for tumors. **B.** Hematoxylin-eosin (H&E) staining of representative tumors from *Sulf2* WT, *Sulf2* Hz KO and *Sulf2* Hm KO mice showed typical HCC. **C.** Bar graphs showed that significantly smaller proportions of *Sulf2* Hm KO and *Sulf2* Hz KO mice presented ≥5 tumors/mouse (top panel) and tumor volume ≥35 $mm^3$ (lower panel) compared with *Sulf2* WT mice. **D.** Bar graph representing lung metastasis incidence (left panel) and H&E staining (right panel) showed that *Sulf2* WT mice developed lung metastasis but *Sulf2* Hm KO did not. **P*< .05; ***P*< .01.

***Figure 2. SULF2 expression promotes angiogenesis in HCCs***

**A.** DEN-induced HCCs from *Sulf2* Hm KO mice had decreased MVD compared to tumors from *Sulf2* WT mice, as shown by CD31 immunohistochemical staining (left panel, 200×) and quantification of tumor microvascular density (right panel). For quantification of MVD, CD31-positive cells were identified by a brown precipitate in the cytoplasm of endothelial cells; vessels in each section were counted in five microscope fields. **B.** VEGFR2 immunohistochemical staining of HCC tumors from DEN-induced *Sulf2* WT and *Sulf2* Hm KO mice showed increased staining in *Sulf2*-expressing tumors (400×). Tumor tissues were fixed in formalin, embedded in paraffin, sectioned and stained with antibody against VEGFR2. **C and D.** Tube formation (C) and chemotaxis (D) of HHSECs and HUVECs, measured after 12 hours treatment with conditioned medium (CM) from high SULF2-expressing Hep3B or low SULF2-expressing Huh-7, showed that the expression status of SULF2 in the CM can affect tumor angiogenesis. **P*< .05; ***P*< .01; ****P*< .001.

***Figure 3. POSTN is a key downstream signaling molecule mediating SULF2 induced HCC angiogenesis.*** **A and B.** Relative mRNA expression of 25 pro-angiogenic factors in (A) Hep3B cells transfected with control or SULF2 overexpressing vectors or (B) Huh-7 transfected with scrRNA or shSULF2. Together, these results showed that POSTN was the most highly correlated gene to SULF2 expression status. **C,D and E.** Relative expression of POSTN at mRNA level (C), protein level (D) and by immunofluorescence staining (E) in Hep3B cells overexpressing SULF2, Huh-7 transfected with siSULF2, and their corresponding controls showed that the expression of POSTN was dependent of the levels of SULF2. **F.** ELISA performed in the CM of the four different group of cells described above showed that SULF2 regulates the secretion of POSTN protein to the medium. **P*< .05; ***P*< .01; ****P*< .001.

***Figure 4. SULF2 modulates paracrine activation of POSTN pathway in endothelial cells***

**A and B.** Immunoblotting analysis (A) and immunofluorescence (B) of POSTN and its signaling molecules p-FAK and p-AKT expressed in HHSECs co-cultured for 48 hours with Hep3B SULF2 or Huh-7 shSULF2 cells and their respective controls, as well as co-cultured with high SULF2-expressing Hep3B cells in which POSTN is targeted by siRNA. **C and D.** Immunoblotting analysis (C) and immunofluorescence (D) of POSTN and its signaling molecules p-FAK and p-AKT expressed in HUVECs co-cultured for 48 hours with Hep3B SULF2 or Huh-7 siSULF2 cells and their respective controls, as well as co-cultured with high SULF2-expressing Hep3B cells in which POSTN is targeted by siRNA.

***Figure 5. SULF2-mediated promotion of angiogenesis is POSTN-dependent***

**A.** HHSECs and HUVECs cells were incubated for 12 hours with CM from SULF2-overexpressing Hep3B cells co-transfected with siPOSTN, and then collected and tested for cell viability, adhesion, chemotaxis and tube formation. Results showed a decrease in the angiogenic potency of the cells when

POSTN expression was donwregulated.. **B**. Representation of the tumor volume of subcutaneous mouse xenografts. Combinations of Hep3B cells infected with adenovirus containing either shSULF2 or control vector (empty vector) along with shPOSTN or scramble control (scrRNA) were injected subcutaneously in the right flank of NOD/SCID mice (6 mice per group). Tumor volume was measured 3 times a week up to the end point of the experiment. **C.** Viability, adhesion and tube formation ability of HHSECs and HUVECs were augmented after treatment with increasing concentrations of recombinant human (rh) POSTN. **D.** Relative mRNA expression of SULF2-associated angiogenic factors in Hep3B SULF2 cells co-transfected with either control siRNA or siPOSTN. Results of immunofluorescence staining confirmed the results of RT-PCR, where the downregulation of the POSTN expression led to a decrease in the expression of angiogenic factors VEGFB, MMP2, MMP9, PDGFA and PDGFB. **P*< .05; ***P*< .01; ****P*< .001.

***Figure 6. SULF2 increases POSTN expression via activation of the TGFβ pathway***

**A.** Immunoblotting of Hep3B cell lysates with low or high SULF2 expression showed inducction of POSTN after recombinant (rh) TGFβ1 treatment along with the activation of the TGFβ1 downstream pathway. **B.** POSTN expression analyzed by RT-qPCR and ELISA in HCC cells with low or high SULF2 expression after TGFβ1 treatment confirmed the results obtained at protein level. **C.** Immunofluorescence showed higher levels of TGFβ1 and POSTN in high SULF2 expressing HCC cells compared to the controls, for both times tested. **D.** Immunoblotting of Hep3B and PLC/PRF/5 cell lysates after treatment with rhTGFβ1 during 0, 24, 48 and 72 hours. Results showed induction of TGFβ1 and POSTN expression in a time dependent manner. **E.** Immunoprecipitation revealed loss of interaction between TGFβ1 and TGFBR3 in Huh-7 cell lysates with high SULF2 expression. **F.** ELISA showed higher concentrations of TGFβ1 in the CM from high SULF2-expressing cells compared with controls, and that the increment is time-dependent. **G.** POSTN expression analyzed by RT-qPCR and ELISA in HCC cells with high SULF2

expression after treatment with rhTGFβ1, in the presence or absence of a TGFβR inhibitor treatment (SB431542). Results showed that the SULF2-mediated stimulation of POSTN is TFGβ1-dependent. **H.** Bioinformatics analysis of the POSTN promoter identified two regions with candidate SMAD (*S*) binding sites upstream of their first exon and primers for q-PCR were design to amplify these sites. ChIP assay performed in Huh-7 cells after 1 hour treatment with 5 ng/mL rhTGFβ1 in the absence of FBS confirmed binding of Smad3 transcription factor to the POSTN gene promoter in the Site#2. **P*< .05; ***P*< .01.

***Figure 7. SULF2 and POSTN are co-expressed in human HCC and associated with poor patient survival***.

**A.** Relative mRNA expression of CD31 and CD34 in HCC specimens. For this analysis, samples have been divided in high SULF2 and low SULF2 expressing tumors. Results, presented as fold of change between HCC tumor and adjacent benign tissues, showed that the mRNA levels of CD31 and CD34 were elevated in high-SULF2 expression than in low-SULF2 expression HCC. **B.** POSTN is overexpressed in a subset of human HCCs and its expression is positively correlated with SULF2 expression. **C.** Patients with HCC tumors expressing high levels of POSTN had a significantly worse prognosis than those with low POSTN expression. **D.** Analysis of The Cancer Genome Atlas (TCGA) data shows that POSTN was significantly overexpressed in tumor tissues when compared to peritumoral benign tissues (left panel) and POSTN expression is positively correlated with SULF2 expression (right panel). **E.** High POSTN expression was confirmed to be associated with poorer overall survival in TCGA dataset. **P*< .05; ****P*< .001.

# Figure 1

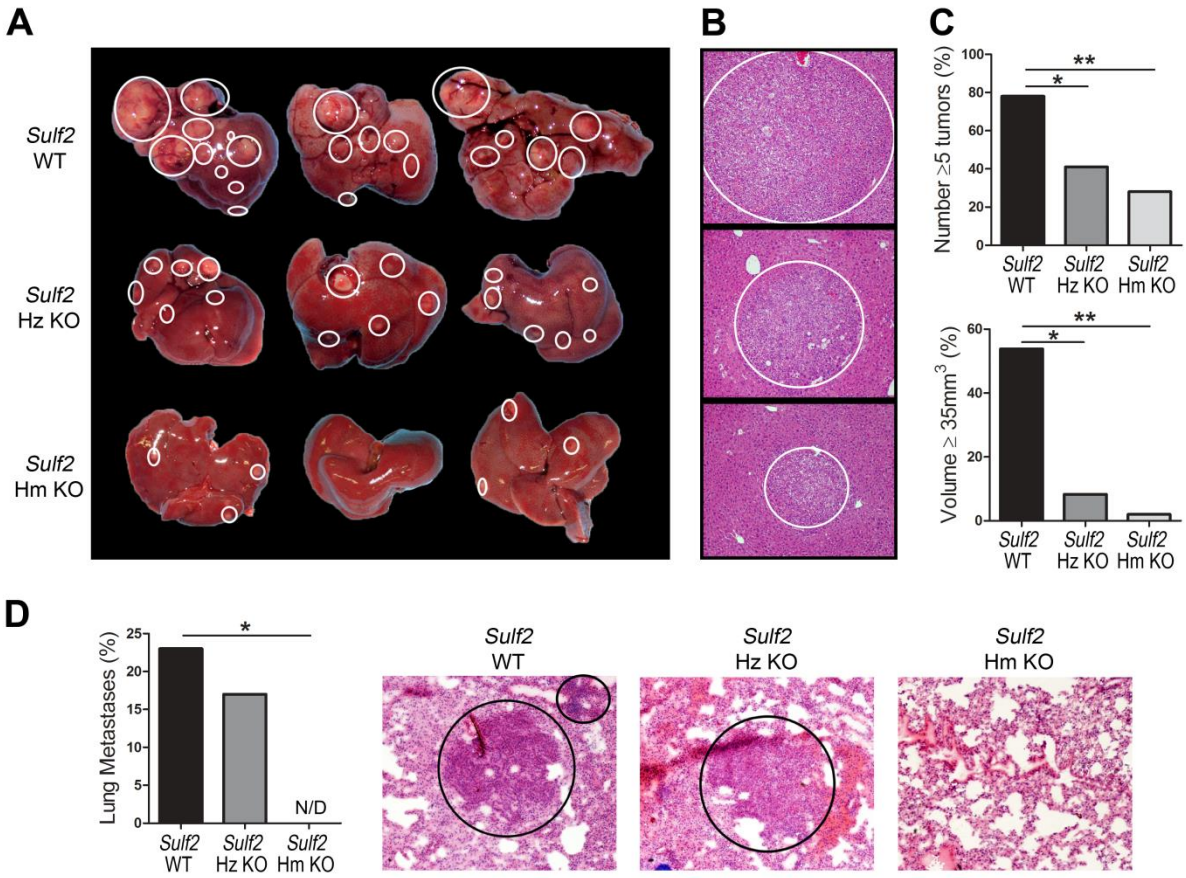

# Figure 2

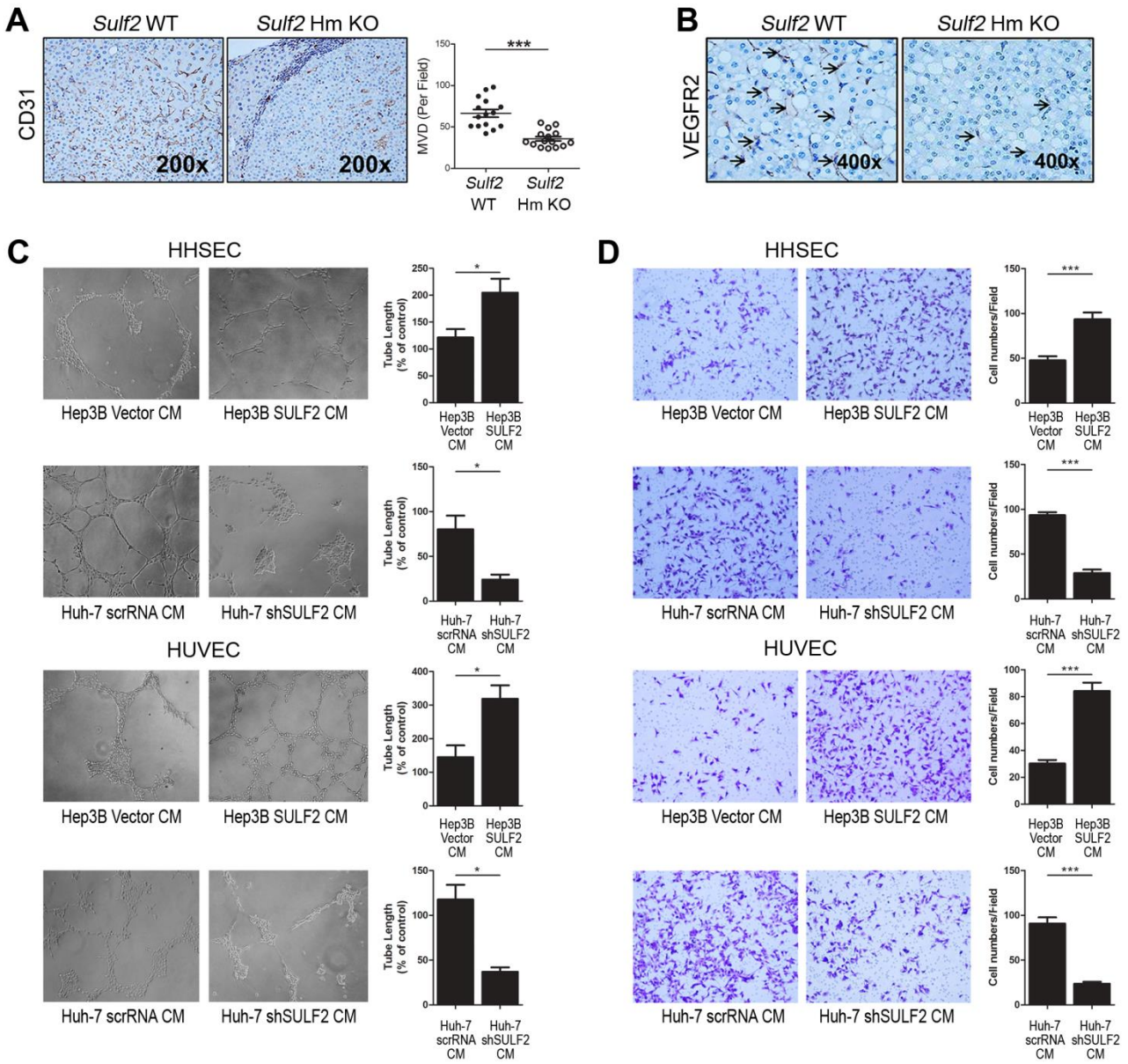

# Figure 3

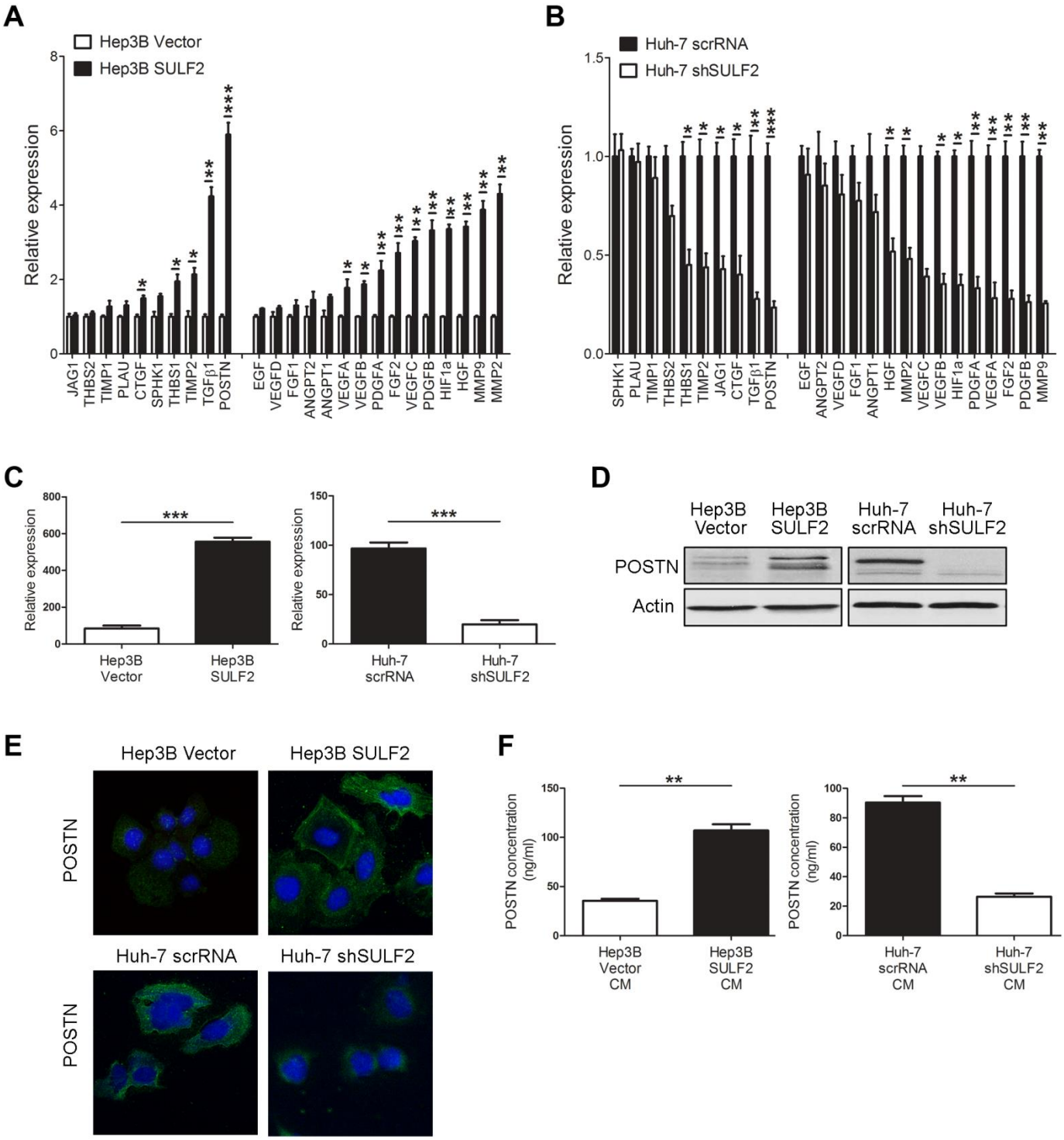

# Figure 4

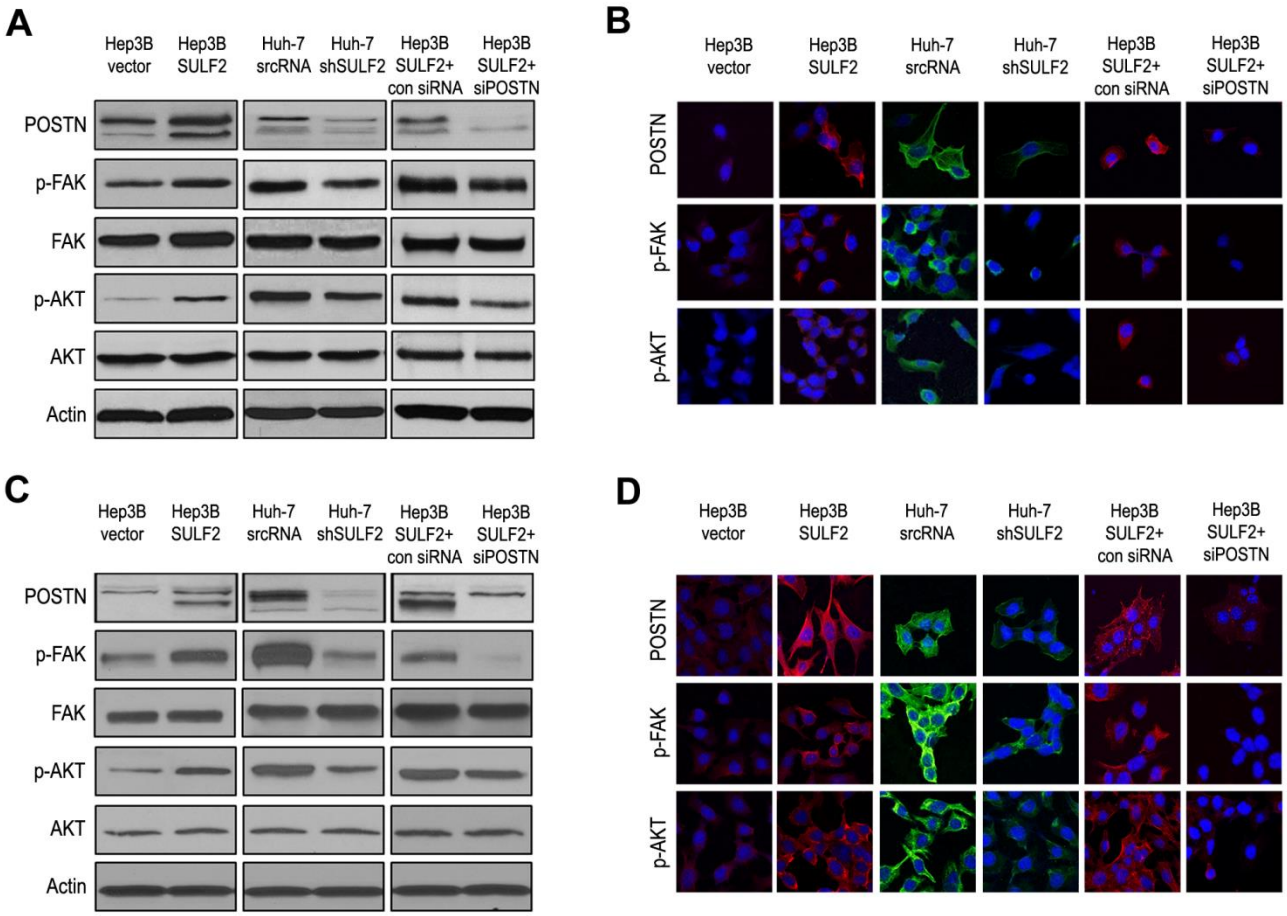

# Figure 5

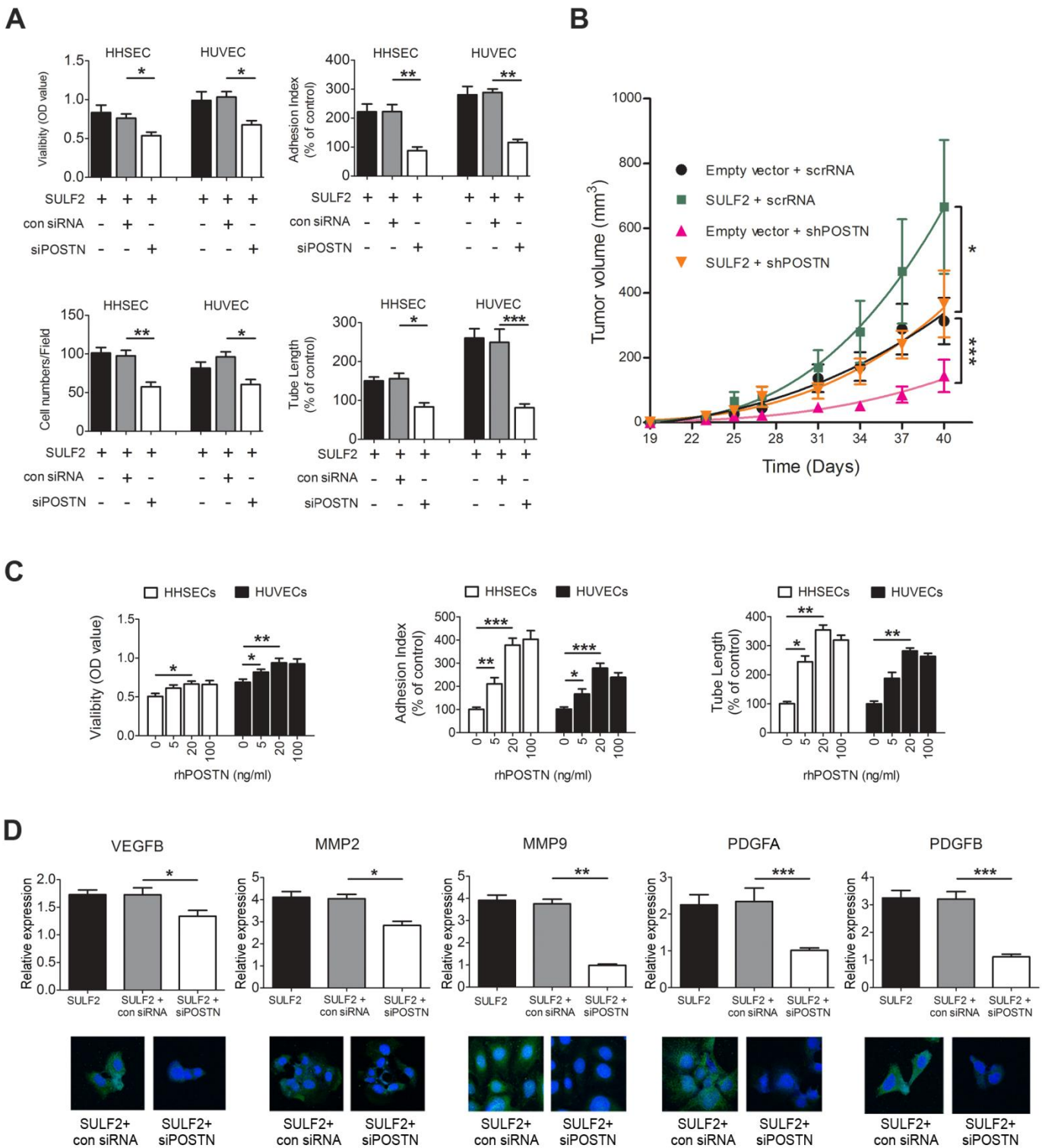

# Figure 6

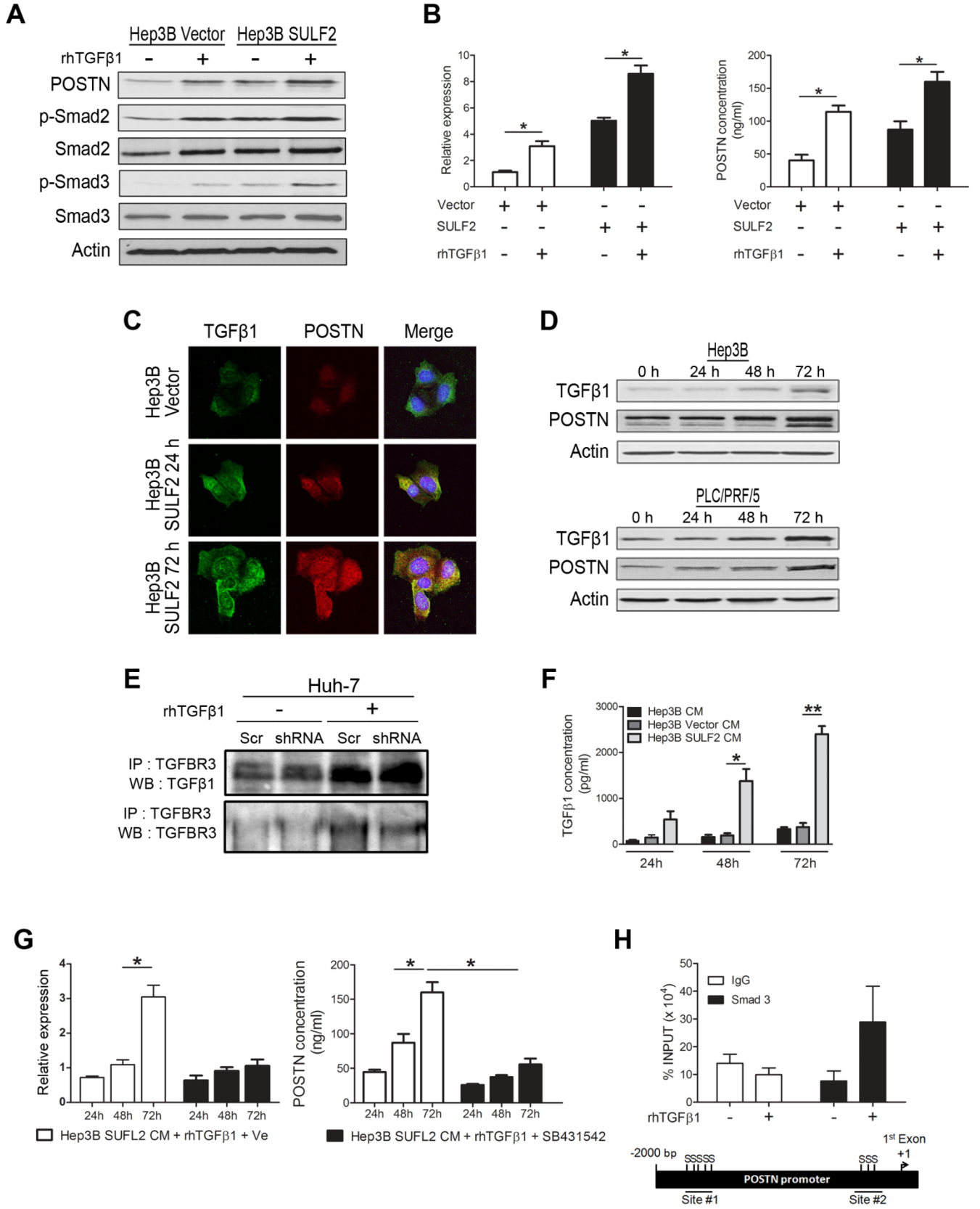

# Figure 7

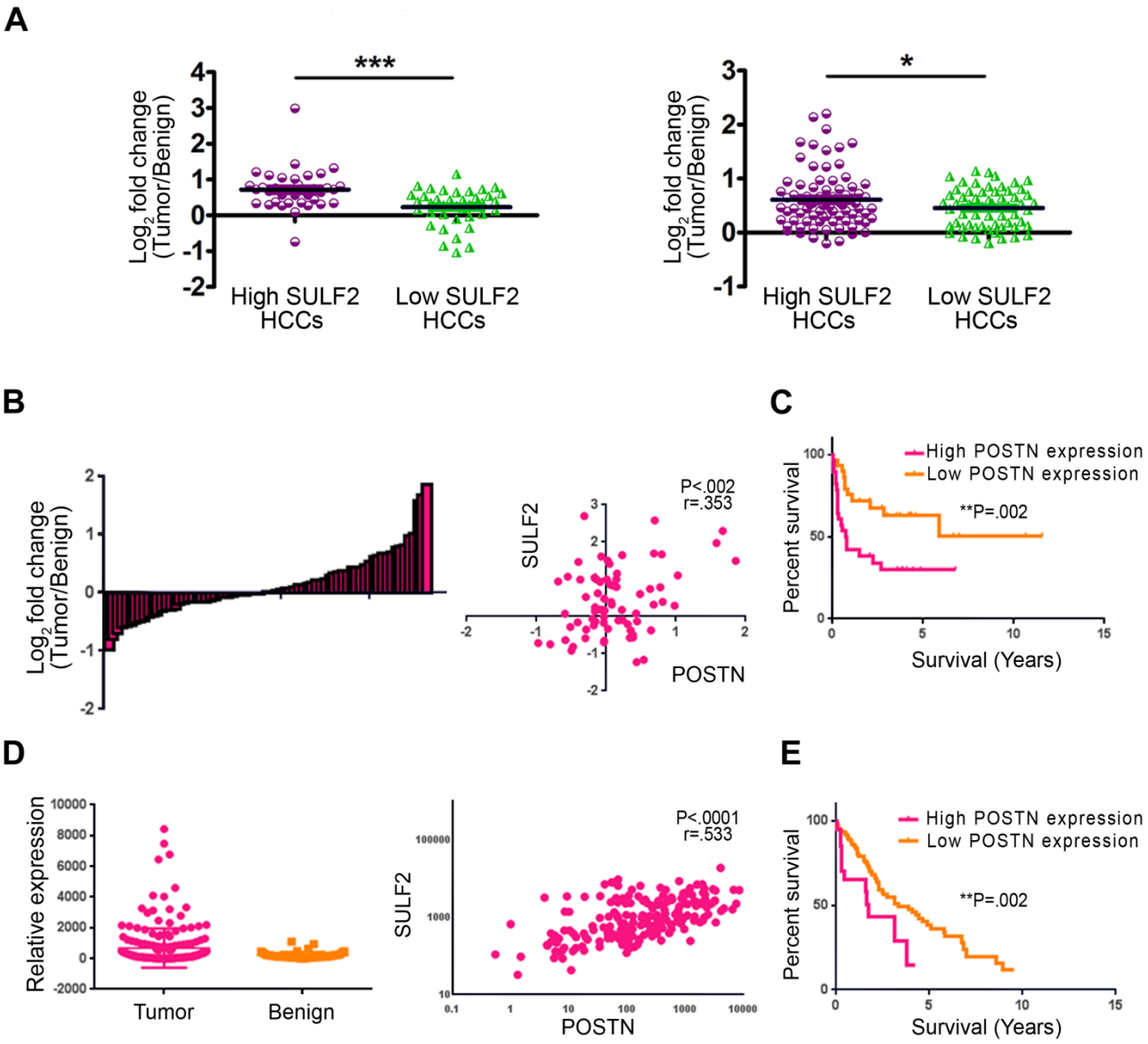

AACR American Association for Cancer Research

Cancer Research

The Journal of Cancer Research (1916–1930) | The American Journal of Cancer (1931–1940)

# Transcriptional induction of Periostin by a Sulfatase 2-TGFβ 1-SMAD signaling axis mediates tumor angiogenesis in hepatocellular carcinoma

Gang Chen, Ikuo Nakamura, Renumathy Dhanasekaran, et al.

*Cancer Res* Published OnlineFirst November 21, 2016.